Anti-icing propylene-glycol materials

Xi Yao [a,b,1], Baohong Chen [a,1], Xavier P. Morelle [a,c], Zhigang Suo [a,*]

[a] *John A. Paulson School of Engineering and Applied Sciences, Kavli Institute for Bionano Science and Technology, Harvard University, MA, 02138, USA*
[b] *Key Lab for Special Functional Materials of Ministry of Education, School of Materials, Henan University, Kaifeng, Henan Province, 475004, PR China*
[c] *Laboratoire d'Ingénierie des Matériaux Polymères, CNRS UMR n° 5223, INSA de Lyon, 69100 Villeurbanne, France*

ARTICLE INFO

ABSTRACT

Liquid propylene-glycol (PG) has long been used as an anti-icing substance, for example, by spraying on an airplane parked in an airport. In applications, large quantities of PG flow away, which is costly and raises environmental concerns. Here we report propylene-glycol materials, including PG-gels and PG-gel/cotton composites. A PG-gel consists of PG molecules as a solvent and a polymer network. PG evaporates slowly, and the polymer network retains the PG molecules so long as the gel is not in contact with running water. Water and PG form a eutectic system with a eutectic temperature of -60 °C. When ice falls on the surface of the gel, the ice and the PG molecules compete for water molecules, and thermodynamics dictates that the ice should lose water molecules to the PG molecules, so that ice melts and water molecules dissolve in the gel. A liquid-like layer exists on the ice/gel interface, the adhesion energy between the gel and ice is low, and ice readily slides on the gel. We peel a PG-gel from ice, and measure a low adhesion energy of $\sim$3 Jm^{-2} at temperatures about -35 °C. We further demonstrate PG-gel/cotton composites as tough, anti-icing blankets. The blankets are reusable if one removes water by dehydration, and replenish PG by submerging the blanket in liquid PG.

© 2021 Elsevier Ltd. All rights reserved.

The accumulation of ice on solid surfaces poses a threat in many situations. Examples include walking and driving [1], taking off and landing of aircrafts [2,3], power lines [4], wind turbines [5], and buildings [6]. Propylene-glycol (PG) has a melting temperature of -55 °C, and forms a liquid solution with water molecules above a eutectic temperature of -60 °C (Fig. 1A) [7]. PG has long been used as anti-icing substance [8,9]. For example, a Boeing 727 requires 35 gallons of PG to prevent the formation of ice, and 150–2000 gallons of PG to remove ice [10]. After such treatments, the plane must depart within 5–15 min [9]. The large quantities of PG flow away, which is costly and raises environmental concerns [11–13].

Here we report propylene-glycol materials, including PG-gels and PG-gel/cotton composites. We prepare a polyacrylic acid (PAA) hydrogel, dehydrate the gel into a dry PAA network, and submerge the dry network in PG (Fig. 1B). The PAA network imbibes PG and forms a PG-gel. PG evaporates slowly, and the polymer network retains the PG molecules so long as the gel is not in contact with running water. At a temperature above about -55 °C, the PG in the gel is in liquid state. When ice falls on the surface of the gel, the ice and the PG molecules compete

for water molecules, and thermodynamics dictates that the ice should lose water molecules to the PG molecules, so that ice melts and water molecules dissolve in the PG gel. A liquid-like layer exists on the ice/gel interface, the adhesion energy between the gel and ice is low, and ice readily slides on the gel. We also prepare a PG-gel/cotton composite as follows (Fig. 1C). A cotton fabric is immersed in the precursor of the PAA hydrogel. The PAA network forms in topological entanglement with the fabric. We dehydrate the composite, and swell the composite in PG. We demonstrate the composite as a tough, anti-icing blanket, reusable by replenishing PG and dehydration.

1. Results and discussion

1.1. Characterizations of PG-gel and PG/water solution

The as-prepared PAA hydrogel is 2 mm thick, and is dried in a homemade chamber. When the dried PAA network is submerged in the pure PG liquid at room temperature, the PAA network imbibes PG and forms the PG-gel. We measure the weight of the PG-gel as a function of time (Fig. 2A). The swelling ratio is defined by the ratio of the weight of PG-gel to the weight of the as-prepared PAA hydrogel. The PG-gel takes around two days to recover the weight of the as-prepared PAA hydrogel and five days to double the weight.

* Corresponding author.
   E-mail address: suo@seas.harvard.edu (Z. Suo).
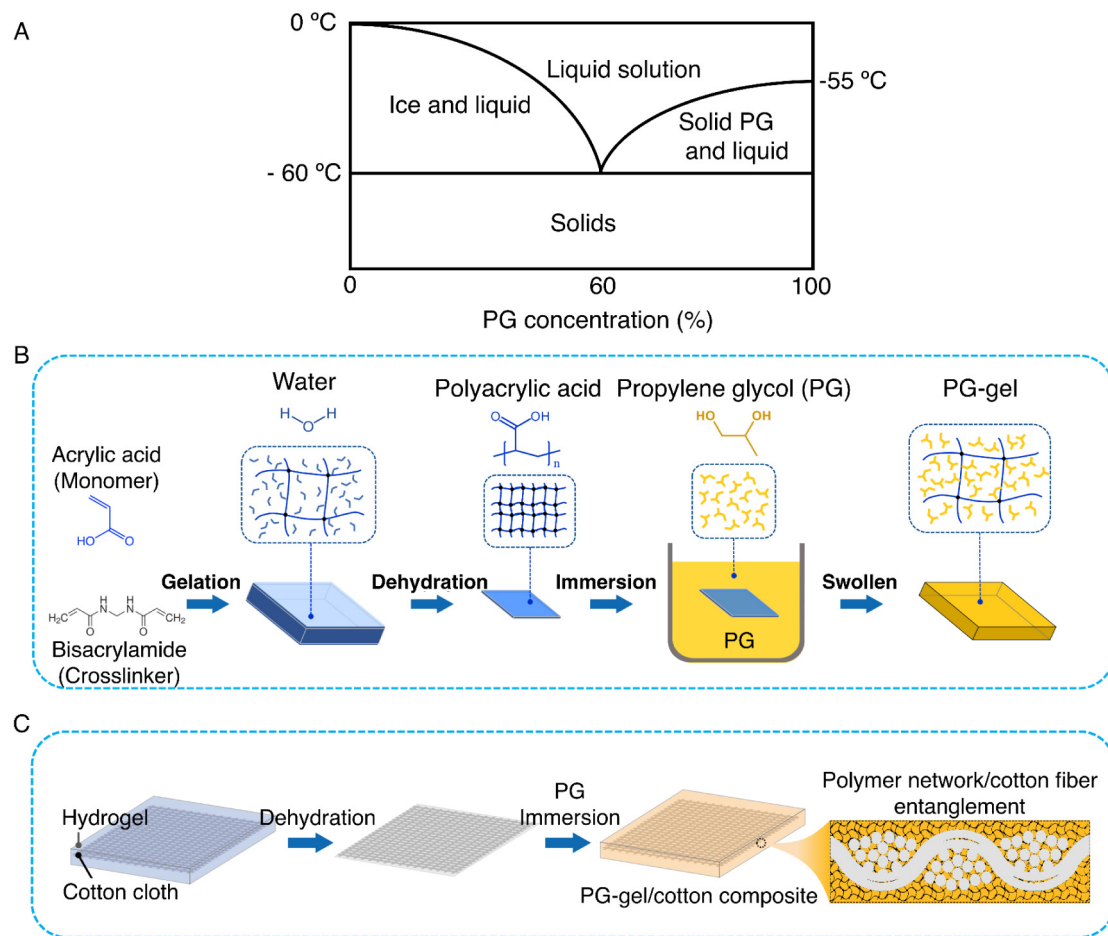[1] These authors contribute equally.

A

B

C

Fig. 1. (A) Schematic PG-water phase diagram. Preparation of (B) PG-gel and (C) PG-gel/cotton composite.

We also submerge a dried PAA network into a PG-water solution for 2 days, and measure the mass ratio of PG over PG and water (Fig. 2B). The PG-to-water ratio in the gel is comparable to that in the solution. We further measure the viscosities of the pure PG and PG/water (mass ratio 3:2) solution at various temperatures (Fig. 2C). The difference in viscosity is dramatic below -10 °C.

We prepare both a PG-gel by submerging a dry PAA in pure PG, and a PG-gel by submerging a dry PAA in a PG-water (3:2) solution for two days. We put the gels on a hot plate at 80 °C in the lab and measure the weight loss as a function of time (Fig. 2D). The pure PG-gel loses weight much slower than the PG-gel containing water, indicating that PG evaporates much slower than water.

Unless otherwise indicated, we will study the pure PG-gel that has the same mass as the as-prepared PAA hydrogel. The PG-gel is sealed in a plastic bag for at least one week at room temperature for homogenization, before subsequent experiments.

1.2. Mechanical properties of PG-gel and PG-gel/cotton composite

We measure stress–stretch curves of the PG-gel at various temperatures (Fig. 2E), and of the PAA hydrogel at two temperatures (Fig. 2F). The elastic modulus of PG-gel is $\sim$10 kPa at room temperature, which is higher than that of PAA hydrogel ($\sim$4 kPa) at room temperature. This difference is likely due to the higher volume faction of polymer in the PG-gel than in the hydrogel gel. Whereas the PAA hydrogel becomes stiffer (modulus $\sim$147 MPa) at -10 °C and fractures at a stretch (λ) less than 1.1, the PG-gel remains soft at -50 °C. Such flexibility at the low temperature

is due to the low freeze point of PG. At lower temperatures, the hysteresis of PG-gel becomes prominent, which is likely due to the high viscosity of PG.

In fabricating a PG-gel/cotton composite, polymer chains are formed in topological entanglement with cotton threads. At a stretch of 1.2, the stress of the PG-gel/cotton composite is over two orders of magnitude higher than that of the PG-gel (Fig. 2G). At room temperature, the toughness is $\sim$100 J m^{-2} for the PAA hydrogel, and is $\sim$2 kJ m^{-2} for the PG-gel/cotton composite. The toughness of the composite increases as temperature drops (Fig. 2H). The extremely high toughness at -80 °C is intriguing, but the detailed mechanism has not been studied at this writing.

1.3. Adhesion toughness between PG-gel/cotton composite and ice

We use 90-degree peel to measure the adhesion toughness between the PG-gel/cotton composite and ice (Fig. 3A). We cool a thermal chamber to a subzero temperature, spray a layer of water on a stainless-steel substrate in the chamber, and place a layer of the composite on top immediately. After one-hour at the same temperature, we use an Instron machine to pull the composite at a constant speed, and record the applied force. The force rises before the peel front advances, and then plateaus when the peel front advances (Fig. 3B and C). The average peel force per width at a plateau gives the adhesion toughness [14]. At a fixed rate of peel, we observe a ductile-to-brittle transition as temperature changes (Fig. 3D). For example, at a rate of peel 50 mm min^{-1}, the adhesion toughness is below $\sim$3 J m^{-2} at a temperature above -35 °C, and rises steeply to $\sim$80 J m^{-2} as temperature
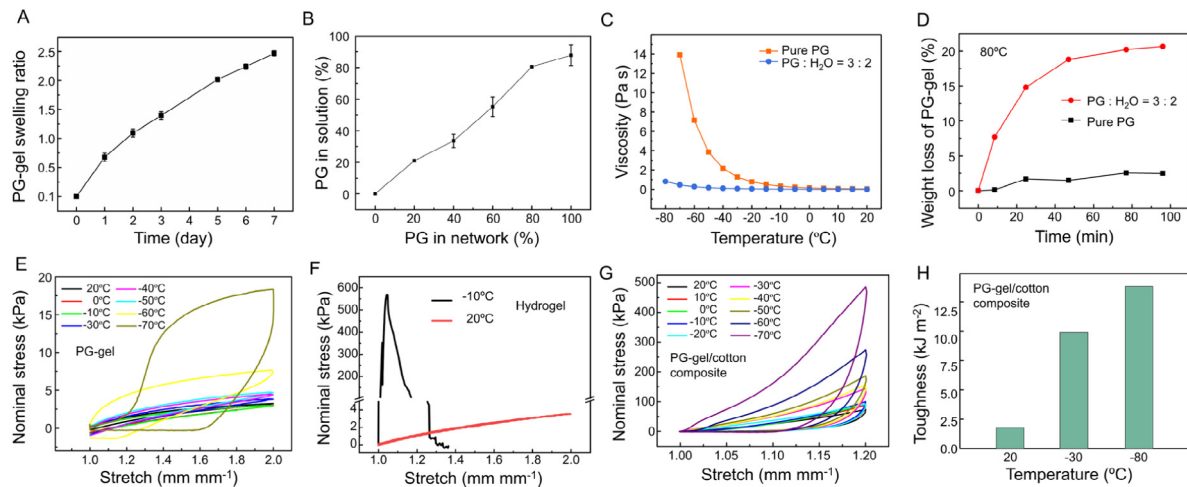
Fig. 2. Properties of PG-gel and PG-gel/cotton composite. (A) Swelling ratio of dry PAA network submerged in pure PG as a function of time. (B) A dry PAA network is submerged in a PG-water solution to swell to equilibrium, and the PG-to-water mass ratio in the gel is the same as that in the solution. (C) Viscosities of pure PG and PG-water (3:2) solution as functions of temperature. (D) Weight losses of pure PG-gel and PG-water (3:2) gel at 80 °C. (E) Stress–stretch curves of a PG-gel at various temperatures. (F) Stress–stretch curves of a hydrogel at two temperatures. (G) Stress–stretch curves of a PG-gel/cotton composite at several temperatures. (H) The toughness of PG-gel/cotton composite at several temperatures.
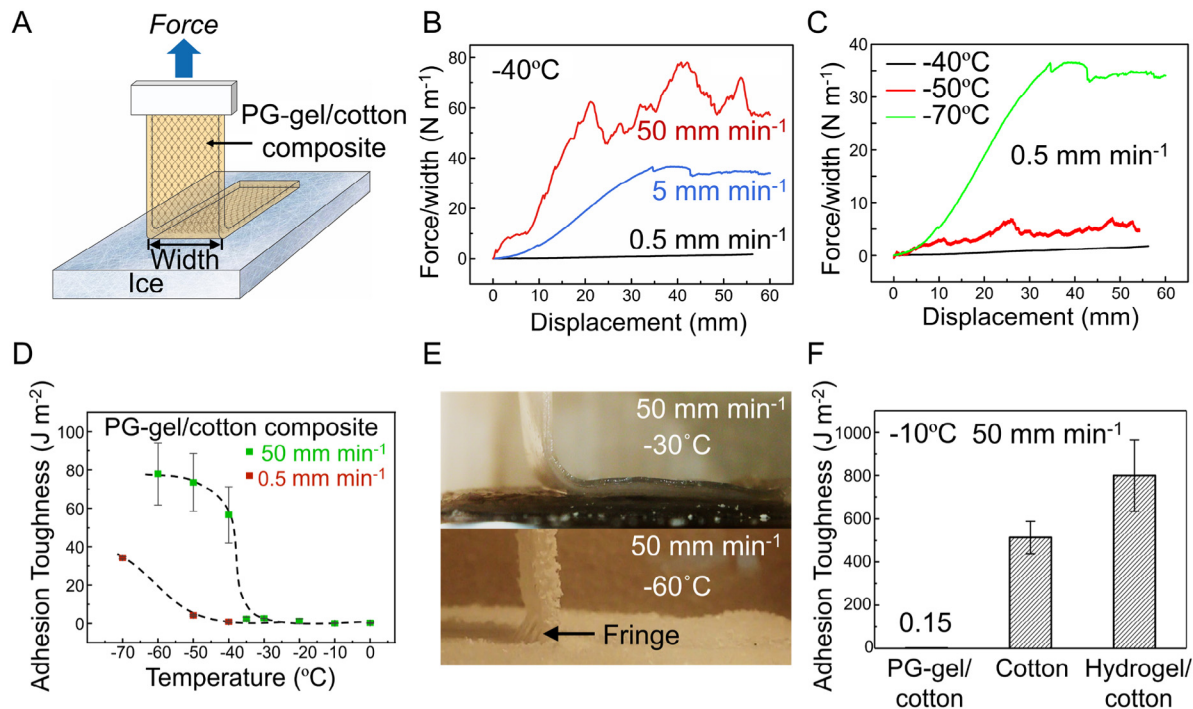

Fig. 3. Peel a PG-gel/cotton composite off ice. (A) Schematic illustration of the 90-degree peel. (B) The force–displacement curves at several rates of peel and at −40 °C. (C) The force–displacement curves at rate of peel 0.5 mm min^{-1} and at several temperatures. (D) The plateau force per unit width defines the adhesion toughness, which is plotted as a function of temperature for two rates of peel, 50 mm min^{-1} and 0.5 mm min^{-1}. (E) Photos of peeling PG-gel/cotton composite at −30 °C and −60 °C, at the rate of peel 50 mm min^{-1}. (F) At −10 °C, the adhesion toughness is measured for three materials: PG-gel/cotton composite, cotton, and hydrogel/cotton composite.

drops further. At a rate of peel 0.5 mm min^{-1}, the ductile-to-brittle transition occurs from −50 °C to −70 °C. We observe the interfacial deadhesion at all temperatures tested. At the rate of peel 50 mm min^{-1}, the peel advances by a straight front at −30 °C, but by a fringed front at −60 °C (Fig. 3E, Supplemental Videos 1 and 2). Also observe that no frost forms on the composite at −30 °C, but frost forms on the composite at −60 °C. At −60 °C and 50 mm min^{-1}, the peel advanced by a fringed front, the fringes retract, and leave a smooth surface. At −10 °C and the rate of peel 50 mm min^{-1}, the adhesion toughness is 0.15 J m^{-2} for the PG-gel/cotton composite, 500 J m^{-2} for the cotton, and 800 J m^{-2}

for the hydrogel/cotton composite (Fig. 3F). These data indicate that the adhesion toughness of ice and PG-gel/cotton composite is low above the ductile-to-brittle transition temperature, and is suitable for deicing applications.

The ductile-to-brittle transition is understood as follows. Above the transition temperature, a thin layer of liquid exists between the ice and polymer network, so that the composite peels off easily. Below the transition temperature, the ice and the polymer network may be connected through a mixture of solid and liquid (i.e., a slush), and the viscosity of the liquid becomes high. Consequently, peel generates a high stress on the interface,

and this high stress may further elicit viscous dissipation in the bulk of the composite. In fact, the measured higher adhesion toughness of ~80 J m^{-2} is larger than the toughness of ice (~20 J m^{-2}) [15,16].

1.4. Transparency at low temperatures

The PG-gel retains a high transparency at a low temperature, which is significant for some anti-icing applications. We place a PG-gel and a PAA hydrogel on a copper substrate (Fig. 4A). Both gels are transparent at room temperature. When the copper is cooled to −30 °C, the PG-gel remains transparent, but the PAA hydrogel becomes opaque.

1.5. Melting of ice on a PG-gel

We use a fluorescent dye to color an ice and watch it melt on a PG-gel. A block of ice, 10 g initially, is placed on a 2 mm-thick PG-gel, and both of them are placed in a freezer at $T = -12.3 \pm 3.4$ °C (Fig. 4B). The ice keeps losing weight over six days, at approximately a constant rate ~1.3 g/day (Fig. 4C). We understand this steady state loss of weight as follows (Fig. 4D). As the ice melts at the ice/PG-gel interface, water molecules diffuse away from the interface, and PG molecules diffuse toward the interface. The molecules further exchange radially in the plane of the gel. The gel has the dimension of 9 cm × 9 cm × 2 mm. The radius of ice is 1 cm. Consequently, the exchange of molecules through the thickness of the gel is faster than the exchange of molecules radially in the plane of the gel. The gel has a high concentration of water within the circle beneath the ice, and a low concentration of water remote from the circle. Because the radius of ice is smaller compared to the size of the gel, the relevant length scale over which molecules exchange is the radius of the ice. Consequently, the molecules exchange in a steady state, and the flux of water across the circumference of the circle in the gel scales as $J \sim D\Delta C/R$, where D is the effective diffusivity of water in the gel, ΔC is the difference in the concentration of water, and R is the radius of the ice. The rate at which the ice loses weight scales as $2\pi RHJ \sim HD\Delta C$, where H is the thickness of the gel. Here $H \sim 10^{-3}$ m. The difference in the concentration of water is estimated by the density of water, $\Delta C \sim 10^6$ g/m^3. The diffusivity is estimated by the Stokes–Einstein relation, $D = kT/6\pi\eta a$, where kT is the temperature in the unit of energy, η is the viscosity, and a is the effective radius of a molecule. Taking representative values, $kT = 4 \times 10^{-21}$ J, $\eta = 1$ Pa s, and $a = 0.3$ nm, we estimate $D \sim 10^{-12}$ m^2/s. These values give an estimation of the rate of weight loss, ~10^{-8} g/s. This value is smaller compared to the observed value of 1.3 g/day ~10^{-5} g/s. The cause of this difference is uncertain at this writing.

1.6. Sliding of ice on an inclined PG-gel

The adhesion and ice melting experiments of PG-gels suggest that the diffusions of PG and water molecules form a lubricant layer of PG-water solution or a slushy layer of PG-H$_2$O mixture throughout the contact area between the PG-gel and ice. Such an interface could facilitate the ice sliding off a curved surface. To investigate the ability of ice removal on the PG-gel by gravity, we design a stage with a tunable inclined angle. The setup is inside a thermal chamber. A sheet of PG-gel is positioned on top of the stage. We spray a thin layer of water on the surface of the PG-gel, and place an ice block on top. Samples and the stage are kept at the same subzero temperature for at least one hour before the test. At −20 °C, we tilt the PG-gel to an angle of 7.8 degrees in 50 s (Fig. 5A). The ice on PG-gel starts sliding immediately at an initial speed of ~35 mm min^{-1} (Supplemental Video 3).

The sliding velocity in 10 s is recorded (Fig. 5B). The measured sliding velocity keeps increasing. At −40 °C, the sliding of ice shows a ~40 min initiation at a speed ~8 μm min^{-1} (Fig. 5C, Supplemental Video 4), although at a larger inclined angle of 45 degrees (Fig. 5A).

1.7. Behavior of H$_2$O molecules on four types of anti-icing materials

We compare four types of anti-icing materials: PG-gel, oil-gel, oil-infused porous material, and superhydrophobic material (Fig. 6). A layer of each material, thickness 2 mm, is placed on a Peltier cooler. The surface of the Peltier cooler is −7 °C when the voltage is turned on. The experiment is conducted in a room at the temperature of 25 °C and at the relative humidity of 60%. On a PG-gel, H$_2$O and PG form a liquid solution (Fig. 6A). Neither water droplets nor ice crystals are observed. The PG-gel is transparent throughout the experiment. This behavior makes the PG-gel a potential anti-icing material in applications in which optical transparency is significant. For example, windows and eyeglasses coated with PG-gels will not accumulate water droplets or frost.

On an oil-gel, H$_2$O molecules dissolve negligibly in the oil, but form water droplets or ice crystals [17,18]. The oil is a liquid at temperatures of anti-icing applications. The adhesion strength between the oil-gel and ice is low [19], indicating that the surface of the gel is oil-rich and the polymer network of the gel adheres negligibly to ice. In our experiment, the oil-gel is transparent initially, but becomes translucent as water droplets accumulate on the surface (Fig. 6B).

An oil-infused porous material has open pores much larger than the polymer mesh size in an oil gel (Fig. 6C). At 15 min, the surface turns translucent as water droplets form. At 30 min, water droplets become large, and ice appears at the edges of the material. After 45 min, ice propagates further towards the center of the surface. Oil does not dissolve H$_2$O molecules, and cannot prevent the propagation of ice from the boundary of the oil-infused porous surface.

On a superhydrophobic surface, small water droplets turn the material translucent at 15 min (Fig. 6D). As time elapses, water droplets become larger, and ice invades from the edges.

1.8. PG-gel/cotton composite, Gore-tex, and cotton fabric

We half-fill three thermoses with water at the temperature of 50 °C, and cover them with PG-gel/cotton composite, porous poly(tetrafluoroethylene) (Gore-tex) cloth, and cotton fabric (Fig. 7). We keep them in a thermal chamber at −30 °C. After 1 h, ice does not accumulate on the PG-gel/cotton composite, but accumulates on both the external and internal surfaces of Gore-tex cloth and cotton fabric. The experiment shows the potential of PG-gel/cotton composites for anti-icing applications, including air-condition, freezer, wind turbine, air source heat pump, and heat exchanger.

1.9. An anti-icing blanket for a model car

We demonstrate the anti-icing blanket made of a PG-gel/cotton composite for vehicles. We use a humidifier to create an icing environment in a thermal chamber at −20 °C (Fig. 8A). Model cars with or without the blanket are placed beneath the humidifier orifice. After one hour, the model car without the blanket accumulates ice (Fig. 8B), but the model car covered with the blanket is ice-free (Fig. 8B). Furthermore, the anti-icing blanket inhibits the adhesion between ice and the blanket, as well as between the model car and the blanket. As we describe before, the blanket is robust, providing an approach of anti-icing operations for vehicles.
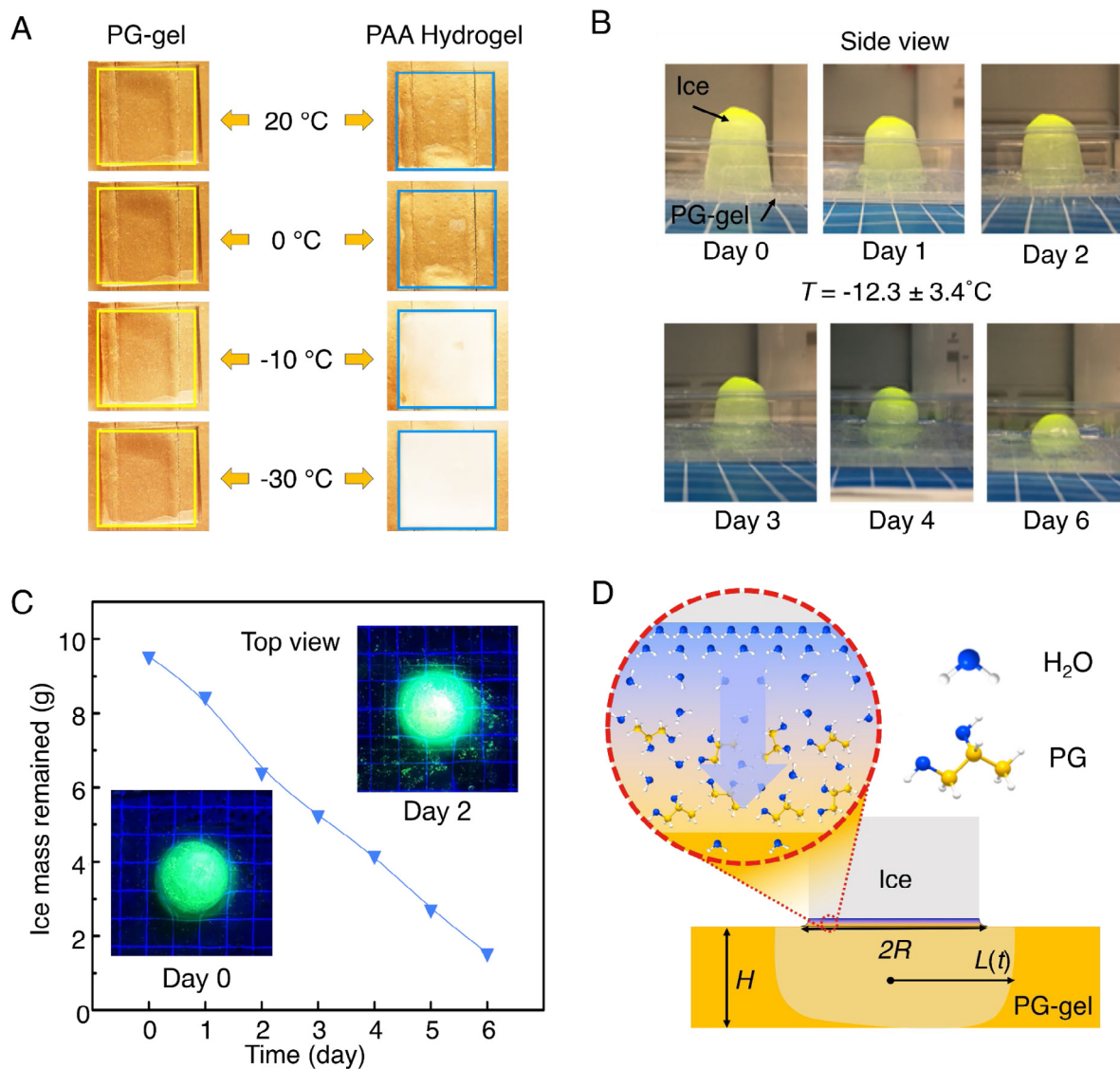
Fig. 4. (A) A PG-gel is transparent at all temperatures, but a hydrogel becomes opaque below 0 °C. (B) On a PG-gel held at −12 °C, a piece of ice (dyed yellow) melts and dissolves. (C) The ice on the PG-gel loses weight as a function of time. Also shown are two fluorescent images of the ice. (D) As the ice melts at the ice/PG-gel interface, water molecules diffuse away from the interface, and PG molecules diffuse toward the interface. (For interpretation of the references to color in this figure legend, the reader is referred to the web version of this article.)
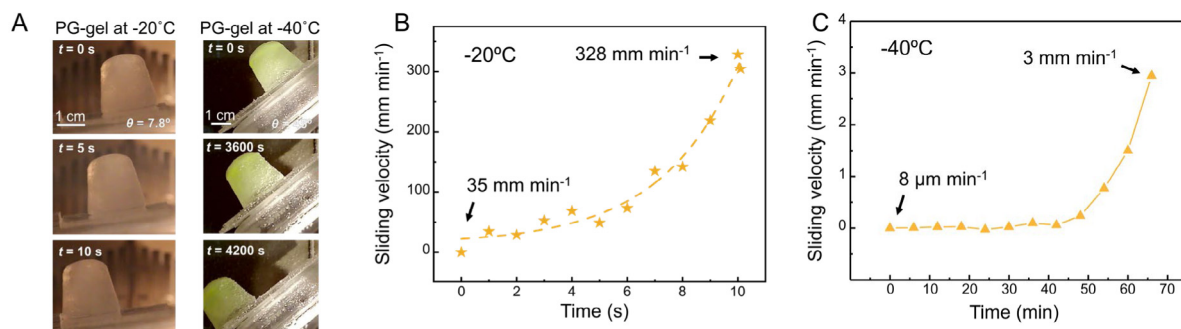

Fig. 5. Ice slides on tilted surfaces. (A) Ice slides on tilted PG-gel surface. At −20 °C, 10 g ice slides immediately on the PG-gel surface when the plate is tilted to ∼7.8° at a rate of 0.156° s⁻¹. At −40 °C, ice slides slowly on the PG-gel surface inclined at a larger angle (∼45°). (B) The sliding velocity of ice on the PG-gel at −20 °C and 7.8° tilt angle. (C) The sliding velocity of ice on the PG-gel at −40 °C and tilt angle of 45 degrees.

The PG-gel/cotton composite can reduce the amount of PG lost in anti-icing applications. Consider a Boeing 727 airplane, of combined area of wings and upper part of the fuselage of

∼400 m². The existing practice is to spray the airplane with ∼138 kg or 600–7800 kg of liquid PG before or after ice forms [10]. By contrast, a PG-gel/cotton composite blanket of 400 m²
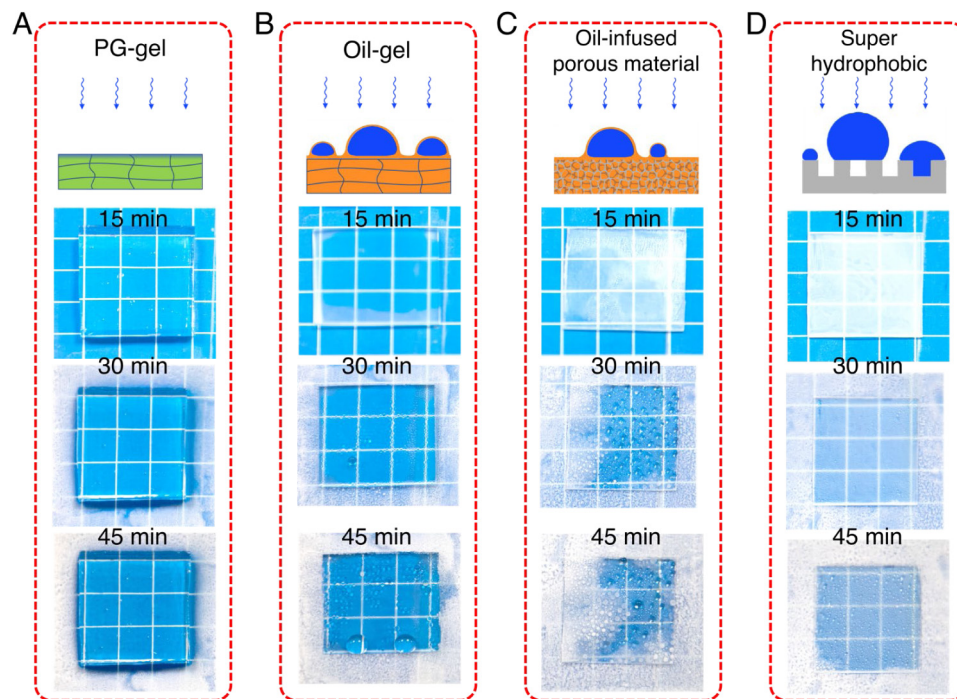
Fig. 6. Behavior of H$_2$O molecules on four types of anti-icing materials: (A) PG-gel, (B) oil-gel, (C) oil-infused porous material, and (D) superhydrophobic material. All four materials are transparent at the beginning of the experiment.
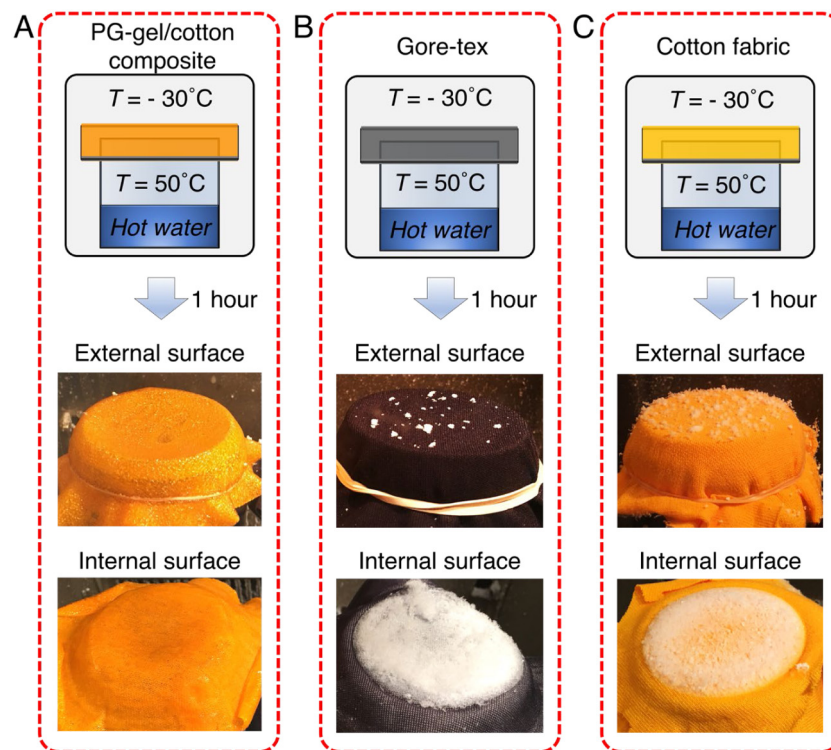

Fig. 7. In a thermal chamber at −30 °C, cups of hot water at 50 °C are covered with three materials: (A) PG-gel/cotton composite, (B) porous poly(tetrafluoroethylene) (Gore-tex) cloth, and (C) cotton fabric. The photos show the external and internal surfaces of each cover after 1 h.

× 1 mm contains ∼416 kg of PG. The PG-gel/cotton composite blanket can be reused. PG has vapor pressure 10 Pa at 20 °C and negligible vapor pressure at subzero temperatures. At subzero temperatures, the blanket loses PG negligibly. The PG inside the gel will not flow to the environment unless the blanket is in contact with running water. After a long-time usage, the gel will

imbibe a large amount of water and lose some PG. One can remove water by dehydration, and replenish PG by submerging the blanket in liquid PG.

In summary, we have reported PG materials with exceptionally weak adhesion to ice above −35 °C. The PG-gel retains a eutectic H$_2$O-PG liquid layer at the interface between ice and the
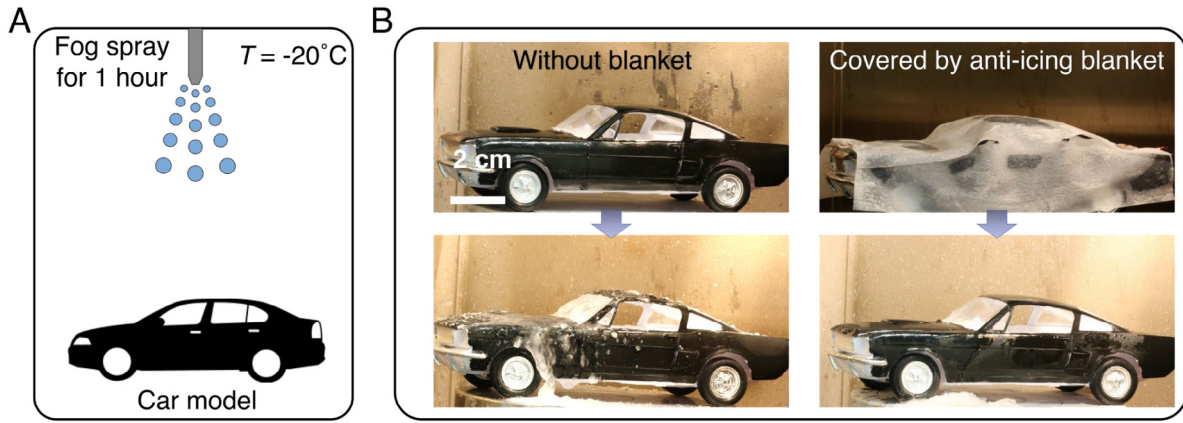
Fig. 8. A PG-gel/cotton composite as an anti-icing blanket. (A) Moisturize a thermal chamber at −20 °C. (B) A model car without the blanket. (C) A model car with blanket.

polymer network. The integration of the PG-gel with cotton fabrics is a convenient way to prepare mechanically robust anti-icing blankets. It is hoped that they will find broad applications.

2. Experiments and methods

2.1. Materials

Acrylic acid (AA, 147230), N,N′-methylenebisacrylamide (MBAA, 146072), and α-ketoglutaric acid (K1750) are purchased from Sigma-Aldrich and used without further purification. Propylene glycol (Purity > 99%), cotton cloth (100% cotton), and model cars are purchased from Amazon.

2.2. The preparation of PG-gel

The preparation starts with the synthesis of the polyacrylic acid (PAA) hydrogel. Acrylic acid (AA) is dissolved in water at a concentration of 2 M. Crosslinker (MBAA) and photo-initiator (-ketoglutaric acid) are added to the AA solution in molar ratios to AA of 0.05% and 0.2%, respectively. The solution is cast into an acrylic mold and sealed by a glass plate on top. The size of the mold is customized according to the requirement of the experiment. PAA hydrogel is cured after 1 h UV irradiation (UVP XX-15L, Analytik Jena). PAA hydrogel is dried in a homemade drying chamber (constant airflow control, velocity ∼10 m s^{-1}). The dehydrated PAA networks are immersed in the pure PG solvent for various amounts of time to obtain the PG-gel. The swelling ratio of a PG-gel is defined by W/W_0, where W is the weight of the PG-gel, and W_0 is the weight of the as-prepared PAA hydrogel.

2.3. PG-gel/cotton composite

The ingredient of PAA precursor for the PG-gel/cotton composite is the same as that for the pure PG-gel. Before the precursor is cast in the acrylic mold, cotton cloth (thickness 0.5 mm) is put in the mold. After the cast, remove all visible bubbles in a vacuum chamber, and seal the mold with a glass plate. The remaining steps are the same as those in preparing PG-gel. Eventually, PG-gel/cotton composite is obtained after the immersion in pure PG liquid.

2.4. PG concentration (inside network vs. bath)

To acquire the composite ratio of PG and water inside a PAA network, we prepare PG-water solutions with various concentrations. (Fig. 2B). PAA hydrogels are prepared and fully dehydrated. The dried network is weighed as W_0. Next, the dried network is immersed in the PG-water solution for two days. After immersion, gels are weighed, marked as W_1. Then restore gels in a desiccator to gradually remove the water in gels. Until the residual weight reaches a plateau, record the weight of gel as W_2. Consequently, the PG concentration inside the gel network is calculated by $(W_2 - W_0)/(W_1 - W_0)$.

2.5. Rheometric (viscosity) test

The rheometric test is conducted on the rheometer (TA-DHR3, USA). The viscosities of the PG and the PG-water solutions are measured at a shear rate of 1 rad s^{-1}.

2.6. Transparency at low temperature

A homemade cooling stage is assembled to observe the change of transparency. The steel stage cooled by ethanol can withstand a temperature as low as −30 °C. Copper tape covers the surface of the stage to give a good heat transfer. A glass box is positioned over the stage with a constant nitrogen flow to prevent the heat exchange with the ambient and eliminate the water condensation on the samples.

2.7. Stretch test

The stretch test is carried out on a test machine (Instron 5966). The samples with a typical gauge sizes (5 cm × 2 cm × 2 mm) are fixed between gripers of the machine.

2.8. Pure shear test

The toughness of the PG-gel/cotton composite is measured through the pure shear test. The sample size between Instron's grippers is 6 cm × 1.5 cm × 3 mm. The loading rate is 50 mm min^{-1}. A 1.5 cm precrack is cut before loading. Critical stretch is recorded when the crack starts to propagate. The toughness is calculated using the energy density of intact sample (without precrack) at critical stretch times the sample height (1.5 cm).

2.9. 90°-peel test

The peel test is conducted in the thermal chamber on Instron with a homemade mechanical accessory. First, the thermal chamber reaches an equilibrium at a desired temperature. Second, spray water to make a thin layer of water on a steel stage in the chamber. Immediately, a sample ($12 \times 2 \times 0.2$ cm^3), e.g. hydrogel/cotton composite, PG-gel/cotton composite, or cotton, contacts the steel stage before the sprayed water turns to ice. One end of the sample is clamped and connected to the load cell through a long copper wire (length > 100 cm). Then the whole setup is retained at the desired temperature for 60 min. During the peel, raise the load cell at fixed velocities.

2.10. Ice melting experiment

The melt of ice is monitored inside a lab freezer with an interior temperature of -12 ± 3.4 °C. A 10 g ice block, made in a kitchen ice mold, is placed on the top of a PG-gel ($5 \times 5 \times 0.2$ cm^3) resting on a plastic (polypropylene) plate. The residual ice is imaged and weighted daily.

2.11. Sliding test

Ice blocks are prepared in a freezer. All ice blocks used in this work have uniform weights of 10 g. An acrylic plate serves as the tilting stage. One end of acrylic plate is fixed on the steel stage inside the chamber, and the other is connected to Instron's moving frame outside the chamber through a copper wire and pulleys. The tilted angle of the acrylic plate is adjusted by moving the frame. Samples are fixed on the acrylic plate. An ice block is positioned on top of the sample. The adhesion of ice on sample is achieved by spray a layer of water in between. Liquid nitrogen is pumped into the chamber and allows the chamber to be set at the desired temperature. The temperature is kept for at least 1 h to enable the thermal equilibrium inside chamber.

2.12. Anti-ice test

A Peltier cooling stage is applied to create a cold surface at -7 °C. Pieces (2×2 cm^2) of PG-gel, superhydrophobic acrylic sheet (treated by "Glaco"), oil gel (PDMS network infused by n-decane), and oil-infused porous material (made of porous Teflon infused by perfluoropolyether, PFPE, Fomblin Y45, Solvay) are positioned on the cooling stage. The samples are exposed in air with a 60% relative humidity and a temperature of 25 °C.

2.13. Cup test

Isothermal cups (Thermos) are half-filled with 50 °C water. The opened cups are covered by different samples on top and fastened with a rubber band. The sample-covered cups are put into the thermal chamber at specific temperatures.

2.14. Model car

The model car is assembled and painted with regular oil-based paint (black). The anti-icing cloak is trimmed based on the PG-gel/cotton composite. The model car with or without a PG-gel cloak rest on the steel stage in the thermal chamber at -20 °C for at least 1 h. Moisture/fog is pumped into the chamber through a silicone tube connected to a commercial humidifier (URPOWER, 5L).

Declaration of competing interest

The authors declare that they have no known competing financial interests or personal relationships that could have appeared to influence the work reported in this paper.

Appendix A. Supplementary data

Supplementary material related to this article can be found online at https://doi.org/10.1016/j.eml.2021.101225.

References

[1] A. Klein-Paste, J. Wåhlin, Wet pavement anti-icing-a physical mechanism, Cold Reg. Sci. Technol. 96 (2013) 1–7.

[2] J. Cole, W. Sand, Statistical study of aircraft icing accidents, in: 29th Aerospace Sciences Meeting, Aerospace Sciences Meetings, American Institute of Aeronautics and Astronautics, Reno, Nevada, U.S.A, 1991.

[3] T. Cebeci, F. Kafyeke, Aircrafticing, Ann. Rev. Fluid Mech. 35 (2003) 11–21.

[4] B. Ruszczak, M. Tomaszewski, Extreme value analysis of wet snow loads on power lines, IEEE Trans. Power Syst. 30 (2015) 457–462.

[5] F. Villalpando, M. Reggio, A. Ilinca, Prediction of ice accretion and anti-icing heating power on wind turbine blades using standard commercial software, Energy 114 (2016) 1041–1052.

[6] M. Carter, R. Stangl, Increasing problems of falling ice and snow on modern tall buildings, CTBUH J. 4 (2012) 24–28.

[7] http://webserver.dmt.upm.es/~isidoro/.

[8] J.R. Rumble, CRC HandBook of Chemistry and Physics, 98th ed., Taylor & Francis Ltd, 2017.

[9] S. Ritter, Aircraft deicers, What's that stuff? 79 (2001) 30.

[10] Preliminary data summary airport deicing operations: Washinton, DC 204602000.

[11] D. Wirthl, R. Pichler, M. Drack, G. Kettlguber, R. Moser, R. Gerstmayr, F. Hartmann, E. Bradt, R. Kaltseis, C.M. Siket, Instant tough bonding of hydrogels for soft machines and electronics, Sci. Adv. 3 (2017) e1700053.

[12] J.R. Fowles, M.I. Banton, L.H. Pottenger, A toxicological review of the propylene glycols, Crit. Rev. Toxicol. 43 (2013) 363–390.

[13] G. Toscano, L. Cavalca, M.Letizia. Colarieti, R. Scelza, R. Scotti, M.A. Rao, V. Andreoni, S. Ciccazzo, G. Greco, Aerobic biodegradation of propylene glycol by soil bacteria, Biodegradation 24 (2013) 603–613.

[14] J. Li, A.D. Celiz, J. Yang, Q. Yang, I. Wamala, W. Whyte, B.R. Seo, N.V. Vasilyev, J.J. Vlassak, Z. Suo, D.J. Mooney, Tough adhesives for diverse wet surfaces, Science 357 (2017) 378–381.

[15] H. Liu, K. Miller, Fracture toughness of fresh-water ice, J. Glaciol. 22 (1979) 135–143.

[16] M. Wenyuan, G. Yingkui, Tilte, Atlantis Press, 2015.

[17] Y. Yu, B. Jin, M.I. Jamil, D. Cheng, Q. Zhang, X. Zhan, F. Chen, Highly stable amphiphilic organogel with exceptional anti-icing performance, ACS Appl. Mater. Interfaces 11 (2019) 12838–12845.

[18] Y. Wang, X. Yao, S. Wu, Q. Li, J. Lv, J. Wang, L. Jiang, Bioinspired solid organogel materials with a regenerable sacrificial alkane surface layer, Adv. Mater. 29 (2017) 1700865.

[19] C. Urata, G.J. Dunderdale, .M.W. England, A. Hozumi, Self-lubricating organogels (SLUGs) with exceptional synersis-induced anti-sticking properties against viscous emulsions and ices, J. Mater. Chem. A 3 (2015) 12626–12630.